Science Journal of Energy Engineering
2020; 8(4): 44-53
http://www.sciencepublishinggroup.com/j/sjee
doi: 10.11648/j.sjee.20200804.11
ISSN: 2376-810X (Print); ISSN: 2376-8126 (Online)

Optimization of Power Transit Through a Double-term Line Term by the UPFC

Mathurin Gogom*, Anedi Oko Ganongo, Nianga Apila, Desire Lilonga-Boyenga

Polytechnic Superior National School Ecole Nationale Superieure Polytechnique, Marien Ngouabi University, Brazzaville, Congo

Email address:
mathuringogom@gmail.com (M. Gogom), okoanedi@gmail.com (A. O. Ganongo), apilanianga@gmail.com (N. Apila), lilongadesire@yahoo.fr (D. Lilonga-Boyenga)

*Corresponding author

To cite this article:
Mathurin Gogom, Anedi Oko Ganongo, Nianga Apila, Desire Lilonga-Boyenga. Optimization of Power Transit Through a Double-term Line Term by the UPFC. *Science Journal of Energy Engineering*. Vol. 8, No. 4, 2020, pp. 44-53. doi: 10.11648/j.sjee.20200804.11

Received: November 19, 2020; **Accepted**: December 2, 2020; **Published**: December 11, 2020

Abstract: Nowadays, transport network of electrical energy operate beyond their thermal limit, due to growing populations, industrialization and modernization needs. To this end, multi-term power lines are erected in order to ensure the transit of the requested energy while ensuring the stability of the electrical network. But when there is loss of one term of these lines for various reasons (short circuits and others), a problem of transit of this energy is posed. Sure, several research works have been the subject of publications in terms of power transit optimization, however the case of the loss of a term of a transmission line is still a challenge. It is clear that when there is a loss of a term of a line, the power transmitted is reduced because of the increase in the impedance of this line. This study proposes an approach that optimizes the transit of electrical energy post-incident. To do this, the use of the third generation FACTS in this case the UPFC allows us to obtain the expected results. The interest of this work is to satisfy even in emergency or post-contingency conditions the demand for electrical energy while ensuring the stability of the system.

Keywords: Optimization, Double Term Electrical Energy, FACTS, Emergency Regime, System Stability, Post Contingency and UPFC

1. Introduction

Electric energy is an essential energy vector for human activities and an essential factor in the development of humanity. And therefore, power grids are key infrastructures that allow this energy to be transported from the production center to the consumption center or to a system of infinite power.

However, the transort of electrical energy is subject to the various problems of voltage drops, joule losses, reactive power transit, overvoltages, voltage imbalances, rotor angle oscillations or transport and losses of a network element (generators, transformers or lines). All of these hazards are known as power grid instability, which you have to understand.

The study of the stability of an electrical network allows to examine behavior the behavior of the network in the face of small or large disturbances. Continuous variations of consumption or production represent only small disturbances. Faults, such as short circuits, loss of a network element (generator, line or transformer) represent major disturbances. The latter are at the origin of the appearance of a difference between mechanical power and electrical power. To have a balance between production and consumption, it is at first sight necessary to increase the number of power stations, lines, transformers, etc., which implies an increase in cost and a degradation of the natural environment [1]. The transient stability and dynamic stability of electrical networks are their ability to ensure synchronous operation of its generators when they are subjected to significant and moderate disturbances. The appearance of such disturbances can lead to large excursions of the rotor angles of some generators or even to the breaking of synchronism which generally develops in a few seconds [1-3].

A variety of approaches allowing the evaluation of the stability of electrical networks has been proposed in the

literature, in particular: indirect numerical integration methods [3], direct energy methods [4-6], probabilistic methods [7, 8], methods based on pattern recognition [8], adaptive nonlinear methods [11] and hybrid methods [9]. Likewise, the means for improving stability have been proposed in the literature, namely: improving stability by conventional means [2], by PSS [13] and by FACTS [12].

In some networks, multi-term power lines are built to transport a large amount of electrical energy. This also honorable technique has limits in the case of loss of a term of the line because of the increase in the impedance of this one, significantly reducing the power to be transported, and therefore a problem of congestion of the line. To pretend to decongest this line, the network may be exposed to the problem of stability of the transport angle during this emergency regime.

The interest of this work is to optimize the transit capacity of the line and the voltage at the interconnection node without veiling the limits of stability of the transport angle in emergency mode. To do this, we will use the indirect method of numerical integration (the theory of equality of areas) which consists in evaluating the transit capacity before, during and after the loss of a term of the line. To optimize the transit capacity and the transport angle, the FACTS device, in this case the UPFC, will be used.

2. Stability of Electrical Networks

2.1. Definitions

For years, various and complex research was carried out to understand the stability problems of power systems. Thus, many definitions of the stability of power systems were offered with emphasis on the various aspects that reflect the manifestation of the stable state of the system. The most recent definition, which we will adopt, is the result of a joint working group (IEEE / CIGRE, 2004).

The stability of a power system is the ability of an electrical energy system, for a given initial operating condition, to return to the same or another state of equilibrium after having undergone a physical disturbance, while maintaining the most of the system variables within their limits, so the entire system remains virtually intact. Thus, a power system having a state of equilibrium is considered to be stable, if following a disturbance, the system returns to the same position of equilibrium. The system is also considered stable if it tends to another position of equilibrium located in the vicinity of the point of initial equilibrium.

2.2. Types of Stability

There are several forms of stability of electrical networks, structured according to Figure 1 below:

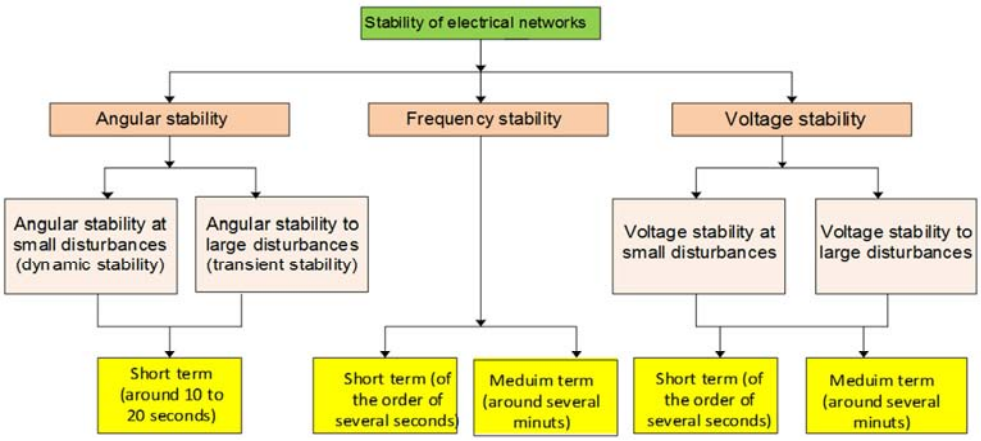

Figure 1. *Different forms of stability.*

2.2.1. Voltage Stability

The voltage stability of an electrical network is the capacity of this network to keep the voltage at each node and at all times within the allowable range. In other words, if after disturbances the voltages at each node of the network are within the allowable range, we say that there is voltage stability. Otherwise, it is said that there is voltage instability which manifests itself in the worst case by a collapse or blackout of the network. There are several types of voltage stability: transient stability due to large disturbances (short circuits or losses of a network element); dynamic stability corresponding to small disturbances (variations in load or production) and static stability (voltage drops or increases in steady state or post-incident regime).

2.2.2. Rotor Angle Stability

It is defined as the ability of a set of interconnected synchronous machines to maintain synchronism under normal operating conditions or after being subjected to a disturbance. Rotor angle instability manifests itself as an increasing gap between the rotor angles of one machine and the rest of the system or group of machines and the rest of the system. A machine which has lost synchronism will be triggered by an over speed protection or by a loss of synchronism protection. Like voltage stability, angular stability manifests itself according to the magnitude of the disturbance; in this dispute, one speaks of angular stability at large disturbances (transient stability), of angular stability at small disturbances (dynamic stability) and of static stability which concerns the permanent

regime or post incident regime.

2.2.3. Frequency Stability

Frequency stability concerns the capacity of the system to keep the frequency close to the nominal value, following a severe incident which may or may not have led to a fragmentation of the system. Frequency stability is closely related to the overall balance between production and consumption. When instability is noted, various frequency adjustments are made. In this dispute, we are talking about the primary adjustment which takes place during the first 15 minutes of the disturbance, of the secondary adjustment after the 15 minutes of the disturbance and of the tertiary adjustment after the 30 minutes of the disturbance.

2.3. Angular Stability Analysis

Angular stability has transient and dynamic aspects. Static stability is often integrated either in the dynamic part corresponding to small disturbances or simply treated as a problem of production-consumption balance. Synchronous machines therefore play an essential role in the analysis of angular stability. Their representation and modelization are therefore the fundamental elements in the analysis of the stability. Since the rotor angle and the transport angle are closely related and can overlap, then the analysis of the transport angle can be inferred from that of the rotor angle. Also, we will not approach this theory without presenting the simplified model of the production system for the analysis of angular stability [10].

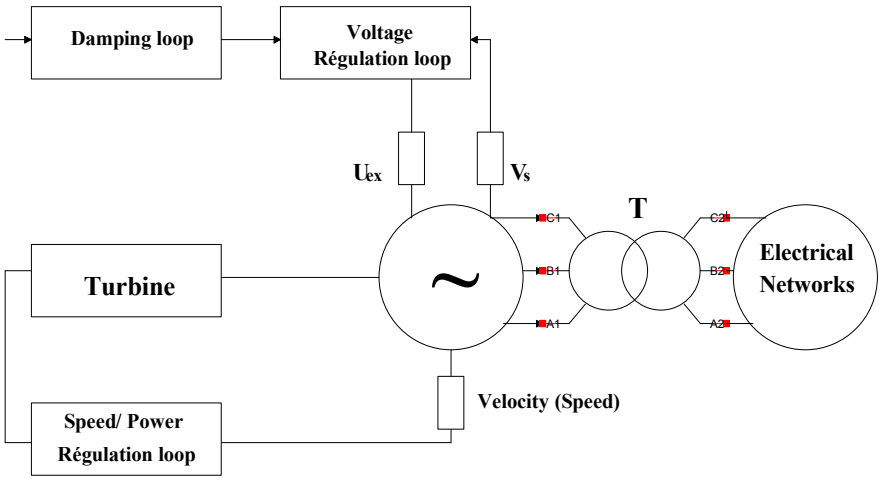

Figure 2. *General diagram of the generator connected to the electrical network.*

2.3.1. Equation of Motion

The basic equations describing the reaction of the rotating masses of synchronous machines to various disturbances are in fact related to the inertia of the synchronous machine and describe the resulting imbalance between the electromagnetic torque and the mechanical torque of these machines. This imbalance can be expressed by the following relation [10]:

$$C_a = C_m - C_e \quad (1)$$

1) C_m: mechanical torque in N.m;
2) C_e: electromagnetic torque in N.m;
3) C_a: acceleration torque in N.m.

This equation applies to both generators and motors. However, for generators, C_e and C_a are positive while for motors they are negative. In the case of generators, C_m represents the mechanical torque produced by the turbine in the direction of rotation (at the level of the machine shaft). It allows therefore the rotor to be accelerated in the positive direction of the rotation. The electromagnetic torque C_e, created by the interaction of the magnetic fluxes of the rotor and the stator, in fact opposes the mechanical torque and corresponds to the electrical power at the level of the air gap of the machine. Under steady-state conditions, the acceleration is zero because $C_m = C_e$. In this case, there is neither acceleration nor deceleration of the moving masses. Thus, the speed is constant and corresponds to the speed of synchronism.

When an imbalance occurs between C_m and C_e, there is an acceleration (or deceleration) of the rotating masses. The latter is expressed as the product of the moment of inertia of these masses by its angular acceleration, which gives:

$$C_a = J\frac{d\omega_m}{dt} = C_m - C_e \quad (2)$$

with

1) J: moment of inertia of all rotating masses (generator and turbine);
2) ω_m: angular speed of the rotor in mechanical radians per second.

In fact, the equation (2) sometimes contains an additional term opposing the mechanical torque. This term includes all the resistive torques corresponding to friction and electromagnetic losses such as the windings of the synchronous machine dampers. This torque also opposes the rotation of mechanical masses. Under these conditions, equation (2) becomes:

$$J\frac{d\omega_n}{dt} = C_m - C_e - \omega_m D_{rm} \quad (3)$$

with D_{rm} the damping torque coefficient.

This additional torque is relatively low and is often neglected compared to the mechanical C_m and electromagnetic C_e torques. However, for some studies, the resistive torque due to the damper windings is taken into account, especially for the study of sustained oscillations.

In what follows and in the context of transient stability, we will not take this additional torque into account. Equation (2) remains in force.

The relation which binds the couples to the powers is given by:

1) $P_m = \omega_m C_m$ mechanical power supplied by the turbine;
2) $p_e = \omega_m C_e$ electromagnetic power.

We then have:

$$J\omega_m \frac{d\omega_m}{dt} = p_m - p_e \quad (4)$$

The coefficient $J\omega_m$ represents the angular momentum of the rotor. We then introduce the notion of relative inertia constant H (in reduced value) frequently used for stability studies. It is defined by the relation:

H= $\frac{\frac{1}{2}J\omega^2 ms}{S_{ref}}$ (kinetic energy of rotating masses at the reference speed) /S_{ref}.

with:

1) ω_{ms}: synchronous angular speed of the rotor in mechanical radians per second;
2) S_{ref}: reference (basic) electrical power of the alternator.

After a few mathematical manipulations, we obtain the final reduced-value equation (pu) below:

$$\frac{2H}{\omega_s}\frac{d^2\delta}{dt^2} = P_m - P_e \quad (5)$$

This equation is known as the equation of motion and is the basis of the analysis of transient angular stability. The solution of this equation for δ, gives us the temporal evolution of this angle, often referred to as the internal angle of the machine, and makes it possible to follow the behavior of the machine with respect to synchronism when a fault occurs in the network. Assuming that $\omega_s = 2\pi f$ where f represents the network frequency, equation (5) becomes:

$$\frac{H}{\pi f}\frac{d^2\delta}{dt^2} = P_m - P_e \quad (6)$$

2.3.2. Rotor Angle or (Transport) Power Considerations in STEADY State

Given the simplified model of the alternator shown in Figure 3 below, the emf induced by the excitation winding is given by:

$$\bar{E} = jX_d\bar{I} + \bar{V_s} \quad (7)$$

X_d being the reactance of the direct axis in steady state. It corresponds to the synchronous reactance.

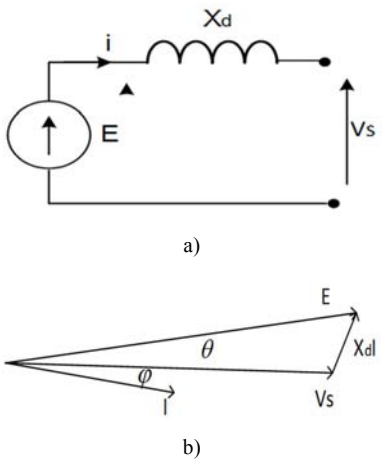

Figure 3. *a) simplified model of an alternator and b) corresponding Fresnel diagram.*

By taking V_s as the phase reference, and the angle δ (internal angle) between E and V_s, we can deduce the complex power per phase:

$$\bar{S} = \bar{V_S}.\bar{I} = \bar{V_S}\left(\frac{\bar{E}-\bar{V_s}}{jX_d}\right) \quad (8)$$

By developing (8), we have:

$$\bar{S} = \frac{V_S E}{X_d}e^{j\left(\frac{\pi}{2}-\delta\right)} - j\frac{V_S^2}{X_d}$$

with

$$\delta = (\vec{E}\hat{}\vec{V_s})$$

We separet the imaginary and real parts, we obtain:

$$\bar{S} = \frac{V_S E}{X_d}\,sin\delta + j\left(\frac{V_S E}{X_d}cos\delta - \frac{V_S}{X_d}\right) \quad (9)$$

we deduce:

1) Active power

$$P = \frac{V_S E}{X_d}sin\delta \quad (10)$$

2) Reactive power

$$Q = \frac{V_S E}{X_d}\cos\delta - \frac{V_S^2}{X_d} \quad (11)$$

Expression (10) therefore corresponds to P_e in the equation of motion. Likewise, expression (11) highlights the link that exists between the reactive power Q and the emf E of the machine and therefore of the excitement. From expression (10), if we increase P_e, by acting on the turbine, while keeping V_s and E constant (X_d remains constant), we see that the angle δ also increases. This maximum power is obtained at the bridge where the angle δ=90°. In these conditions:

$$P_{max} = \frac{V_S E}{X_d}$$

This limit is better known as the static stability limit. Indeed, if the machine is called upon to increase its output power while it is at the P_{max} point, it will no longer be able to remain

synchronized with the rest of the network. Figure 4 below schematizes this characteristic P=f (δ).

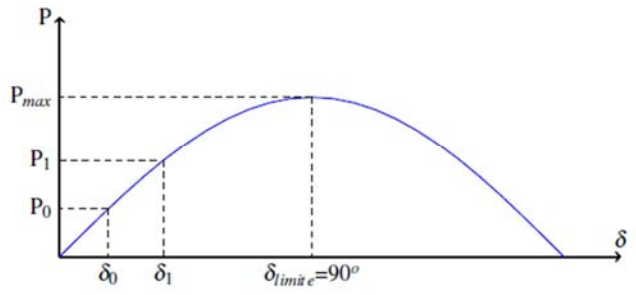

Figure 4. *Variations of P_e as a function of δ.*

2.3.3. Dynamic Analysis

We examine the case where the synchronous machine connected to a network of infinite power experiences small variations in the load. For illustration purposes, the actions of various regulations will not be considered. The initial equation (5) is then written as [10]:

$$\frac{2H}{\omega_s}\frac{d^2\delta}{dt^2} = P_m - P_e = P_m - P_{max}sin\delta \quad (12)$$

This equation highlights a nonlinear relationship between the equation of motion and the internal angle δ. However, for small disturbances resulting in small movements, we can examine the behavior of the machine by linearizing the motion equation around the equilibrium position of the machine rotor. This point is represented by δ_0 such that:

$\delta = \delta_0$ and $P_m = P_e$. So it follows:

$$\frac{2H}{\omega_s}\frac{d^2\Delta\delta}{dt^2} = \Delta P_m - \Delta P_e$$

This equation therefore expresses the effect of the deviation from the equilibrium position. Considering the constant mechanical power, we will have $\Delta P_m = 0$. For low values of Δδ, the difference in the electrical power becomes:

$$\Delta P_e = -P_{max}\sin(\delta_0 + \Delta\delta) \cong -P_{max}cos\delta_0.\Delta\delta \quad (13)$$

We will then have:

$$\frac{2H}{\omega_s}\frac{d^2\Delta\delta}{dt^2} = -P_{max}cos\delta_0.\Delta\delta \quad (14)$$

The equation to be solved is therefore:

$$\frac{2H}{\omega_s}\frac{d^2\Delta\delta}{dt^2} + P_{max}cos\delta_0.\Delta\delta = 0 \quad (15)$$

It is a 2nd order equation in Δδ which has solutions of the form e^{rt}. Always considering that the losses are negligible, for the movement to be stable the response must be decreasing, that is to say, $r^2 \leq 0$. We then have two roots in the complex plane and the movement becomes oscillatory but damped. Otherwise, that is to say, $r^2>0$, the response is exponentially increasing which induces a loss of stability.

2.3.4. Transient Analysis

We are developing here the area equality method, because it is the case of a group of machines connected to a network of infinite power. It is based on the exploitation of Figure 4 to predict the stability of the system following a disturbance. Indeed, the energy stored in the rotating masses of machines can be interpreted graphically in Figure 4 before and after the disturbance. This method is therefore important to understand the bases of the phenomena related to transient stability.

Consider again a synchronous machine connected to a network of infinite power through a line. The phenomena occurring in the synchronous machine before, during and after the disturbance are at the heart of this analysis. The transients in question are considered very fast and the various regulations of the machine have not acted. From the equation of motion (5), we can deduce:

$$\frac{d^2\delta}{dt^2} = \frac{\omega_s}{2H}(P_m - P_e) \quad (16)$$

By multiplying the two sides of this equation by the term $2\frac{d\delta}{dt}$, we will have:

$$\left[2\frac{d\delta}{dt}\right]\frac{d^2\delta}{dt^2} = \frac{\omega_s}{2H}(P_m - P_e)\ \left[2\frac{d\delta}{dt}\right]$$

This equation can be written in the form:

$$\frac{d}{dt}\left[\left(\frac{d\delta}{dt}\right)^2\right] = \frac{\omega_s}{H}(P_m - P_e)\ \frac{d\delta}{dt} \quad (17)$$

Integrating this equation gives us:

$$\left[\left(\frac{d\delta}{dt}\right)^2\right] = \frac{\omega_s}{H}\int_0^{\delta}(P_m - P_e)\,d\delta \quad (18)$$

And therefore:

$$\left(\frac{d\delta}{dt}\right) = \sqrt{\frac{\omega_s}{H}}\int_0^{\delta}(P_m - P_e)d\delta \quad (19)$$

The variation of the speed (with respect to the speed of synchronism expressed by the term $\frac{d\delta}{dt}$ is initially zero (equilibrium position)). The position of the internal angle δ corresponding to this initial position is designated by δ_0. When the system undergoes a disturbance, the imbalance between the mechanical power and the electrical power expressed by the term $(P_m - P_e)$ will induce a change in the term $\frac{d\delta}{dt}$ and therefore a deviation in the internal angle δ. However, for stability to be assured, the term $\frac{d\delta}{dt}$ must become zero once the disturbance has disappeared. One thus deduces a criterion for the stability such that:

$$\left(\frac{d\delta}{dt}\right) = 0 \Longrightarrow \int_{\delta_0}^{\delta}(P_m - P_e)d\delta = 0$$

To better understand this equation, we will illustrate it on a graph representing the curve $P = f(\delta)$. To do this, consider again Figure 4 but taking into account a form of disturbance such as an increment in mechanical power. In this example, the initial operating point corresponds to an internal angle

$\delta = \delta_0$ and $P_{mo} = P_{eo}$. This initial point is represented in the graph of figure 5 by the point "a". So when the mechanical power undergoes a sudden change, it goes from an initial state P_{mo} to a new state P_{ml}, figure 6. An imbalance then occurs

between the mechanical power and the electrical power. As the mechanical power P_{ml} of the new state is greater than the electric power, the resulting acceleration power P_a becomes positive and the rotor is accelerated. However, given the mechanical inertias, the angle δ cannot instantly adjust. The angle δ therefore remains at its initial position δ_0 at the very first moments of the disturbance, which is reflected in the graph of figure 5 by an instantaneous passage from point "a" to point "a' ". The rotor, by accelerating, generates an increase in the angle δ going from δ=δ_0 to δ=δ_1 corresponding to point "b" of equality between the mechanical power and the electrical power. The excess energy stored during this acceleration phase can be expressed by:

$$\int_{\delta_0}^{\delta_1}(P_m - P_e)d\delta = aire(aa'b) = aire\ A_1 \qquad (20)$$

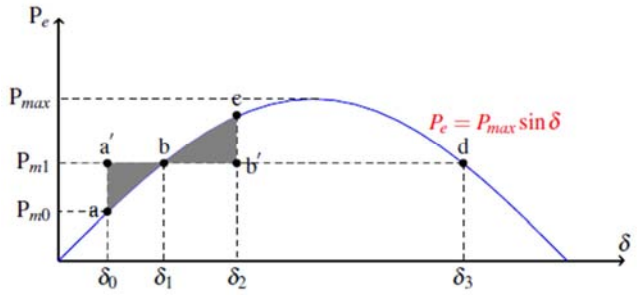

Figure 5. *Graphic representation of the area equality method.*

However, stabilization is not yet achieved because although the acceleration is theoretically zero, the speed of the rotor is greater than the speed of synchronism. The rotor therefore cannot stop at point "b" because of mechanical inertia. The angle δ then continues to increase. But for values of $\delta > \delta_1$, the mechanical power becomes less than the electric power and the acceleration power becomes negative. The rotor then begins to slow down to return to synchronous speed until the stabilization point "b" is reached. During this phase the excursion of the angle δ can go up to a maximum value of $\delta = \delta_2$. The rotor thus loses the energy it has accumulated during the acceleration phase. The return to point "b" is accompanied by oscillations around this point (between δ_0 and δ_2). The various damping elements present in the machine allow these oscillations to be damped to finally stabilize at $\delta = \delta_1$. which will then correspond to the new stable equilibrium state.

During the deceleration phase of the rotor, the energy lost (or restored) is:

$$\int_{\delta 1}^{\delta_2}(P_e - P_m)d\delta = aire(bb'c) = aire\ A_2 \qquad (21)$$

For a system in which we have neglected losses and depreciation, the energy accumulated during the acceleration phase is equal to that lost during the deceleration phase. The corresponding areas are then equal $(A_1 = A_2)$. This is the criterion of equality of areas. If δ_2 is not known, the area A_2 can be calculated by:

$$\int_{\delta 1}^{\pi-\delta_1}(P_e - P_m)d\delta = area\ (bb'c) = area\ A_2 \qquad (22)$$

Under these conditions $(A_1 < A_2)$ to confirm that the system is stable at an adopted degree of compensation.

3. Applications

The contribution to the study of angular stability is applied to the Congolese network, which will incorporate the FACTS of type UPFC in order to optimize the transit capacity of electrical energy and the voltage at the connection node.

3.1. Description and Operation of the UPFC

The UPFC consists of two transformers T1 and T2 used to provide galvanic isolation and adjust voltage levels in the power system, two PWM (Pulse Width Modulation) controlled inverters and a common circuit (capacitor bank). One transformer is connected in parallel and the other in series with the transmission line, Figure 6 [14, 17]. It can be installed at the start or end of the transmission line.

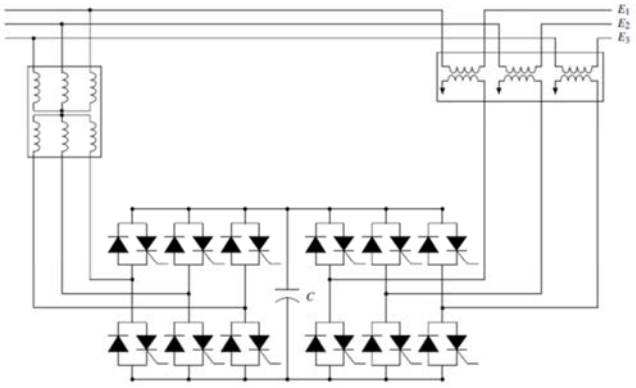

Figure 6. *Block diagram of the UPFC.*

3.2. Description of the Electrical Network

The power grid in Figure 7 consists of a power station connected to the high-power electrical system through two transformers in parallel in series with the double-term line. The electrical system represents the existing Congolese grid considered as load, and the power plant being the new production infrastructure.

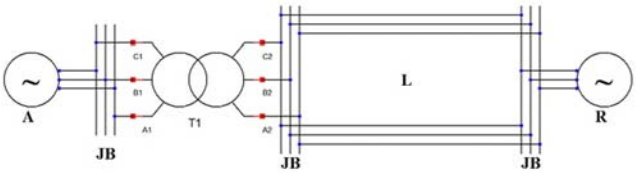

Figure 7. *Schematic diagram of the electrical network.*

where:
A designates all the alternators of the power plant;
JB is the busbars;
L denotes the double term line;
R denotes the infinite power network.

3.3. Modeling of the UPFC and the Electrical Network

3.3.1. Modeling of the UPFC

The simplified circuit of the UPFC control and compensation system is shown in Figure 8. The modeling of this circuit is based on the following assumptions [14, 17]:

1. All switches are assumed to be ideals;
2. The three voltages of the alternative source are balanced;
3. All voltage drops in the series compensator are represented by resistance r;
4. All voltage drops in the parallel compensator are represented by resistance r_p;
5. Harmonics caused by the opening and closing action of switches are neglected.
6. The line inductance L_s plus the leakage inductance of the T2 series transformer are represented by the inductance L;
7. The leakage inductance of the shunt transformer is represented by the inductance L_p.

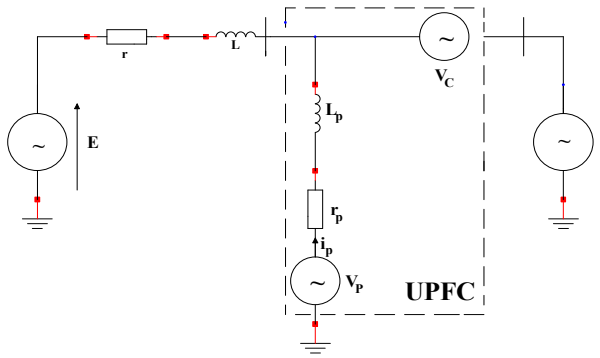

Figure 8. *UPFC model.*

The UPFC controls [14, 17, 18]:

1. the injected voltage V_c in phase with the voltage V_r of the line.
2. the line impedance, the injected voltage being in quadrature with the line current I_r.
3. the voltage phase or the transport angle.

The main purpose of these three operating modes is to control the active and reactive power passing through the line. In addition, the UPFC is able to combine serial and parallel compensation and switch from one operating mode to another.

(i) Modeling of the Parallel Part of the UPFC

The dynamic equations of the parallel part of the UPFC are obtained by applying KIRCHHOFF's laws relating to the three phases [14, 17, 18]:

$$\begin{cases} \frac{di_{pa}}{dt} = -\frac{r_p}{L_p} i_{pa} + \frac{1}{L_p}\left(V_{pa} - V_{ca} - V_{ra}\right) \\ \frac{di_{pb}}{dt} = -\frac{r_p}{L_p} i_{pb} + \frac{1}{L_p}\left(V_{pb} - V_{cb} - V_{rb}\right) \\ \frac{di_{pc}}{dt} = -\frac{r_p}{L_p} i_{pc} + \frac{1}{L_p}\left(V_{pc} - V_{cc} - V_{rc}\right) \end{cases} \quad (23)$$

Where $I_{p,abc}$ the currents of the UPFC shunt are, $V_{p,abc}$ are the voltages generated by inverter 1, r_p and L_p are the resistance and inductance of the UPFC shunt respectively.

The system of equations (21) can be rewritten in the matrix form (22):

$$\begin{bmatrix} V_{pa} \\ V_{pb} \\ V_{pc} \end{bmatrix} = \begin{bmatrix} r_p + s.L_p & 0 & 0 \\ 0 & r_p + s.L_p & 0 \\ 0 & 0 & r_p + s.L_p \end{bmatrix} \begin{bmatrix} i_{pa} \\ i_{pb} \\ i_{pc} \end{bmatrix} + \begin{bmatrix} V_{ca} + V_{ra} \\ V_{cb} + V_{rb} \\ V_{cc} + V_{rc} \end{bmatrix} \quad (24)$$

Of which i_{pa}, i_{pb} *and* i_{pc} represent the shunt currents, moreover V_{pa}, V_{pb} *and* V_{pc} are the voltages generated by the shunt inverter. In matrix form the system (21) become

$$\frac{d}{dt}\begin{bmatrix} i_{pa} \\ i_{pb} \\ i_{pc} \end{bmatrix} = \begin{bmatrix} -r_p/L_p & 0 & 0 \\ 0 & -r_p/L_p & 0 \\ 0 & 0 & -r_p/L_p \end{bmatrix} \begin{bmatrix} i_{pa} \\ i_{pb} \\ i_{pc} \end{bmatrix} + \frac{1}{L_p}\begin{bmatrix} V_{ca} + V_{ra} \\ V_{cb} + V_{rb} \\ V_{cc} + V_{rc} \end{bmatrix} \quad (25)$$

(ii). Modeling of the Serial Part of the UPFC

By applying Kirchhoff's laws to the serial part of the UPFC in figure 9, we will have the following equations [14, 17, 18]:

$$V_s - rI_s - L\frac{di_s}{dt} - V_c - V_r = 0$$

$$-rI_s - L\frac{di_s}{dt} = V_c + V_r - V_s$$

$$L\frac{di_s}{dt} = -ri_s + V_s - V_c - V_r$$

From where:

$$\frac{di_s}{dt} = -\frac{r}{L} i_s + \frac{1}{L}(V_s - V_c - V_r)$$

By writing for the three phases, we have:

$$\begin{cases} \frac{di_{sa}}{dt} = -\frac{r}{L} i_{sa} + \frac{1}{L}(V_{sa} - V_{ca} - V_{ra}) \\ \frac{di_{sb}}{dt} = -\frac{r}{L} i_{sb} + \frac{1}{L}(V_{sa} - V_{cb} - V_{rb}) \\ \frac{di_{sc}}{dt} = -\frac{r}{L} i_{sc} + \frac{1}{L}(V_{sc} - V_{cc} - V_{rc}) \end{cases} \quad (26)$$

The system of equation (23) can be rewritten by the following expression:

$$\begin{bmatrix} V_{sa} \\ V_{sb} \\ V_{sc} \end{bmatrix} = \begin{bmatrix} r + s.L & 0 & 0 \\ 0 & r + s.L & 0 \\ 0 & 0 & r + s.L \end{bmatrix} \begin{bmatrix} i_{sa} \\ i_{sb} \\ i_{sc} \end{bmatrix} + \begin{bmatrix} V_{ca} + V_{ra} \\ V_{cb} + V_{rb} \\ V_{cc} + V_{rc} \end{bmatrix} \quad (27)$$

(iii) Modeling of the Continuous Branch of the UPFC

Based on the principle of power balance and neglecting the losses in the converters, the direct voltage V_c is deduced by the following equation [14, 17, 18]:

$$\left(\frac{1}{2}\right).\frac{dV_c}{dt} = \frac{1}{c.V_{dc}}.\left(P_e - P_{ep}\right) \quad (28)$$

with

$$P_e = V_{ca}.i_{ra} + V_{cb}.i_{rb} + V_{cc}i_{rc}$$

$$P_{eb} = V_{pa}.i_{pa} + V_{pb}.i_{pb} + V_{pc}i_{pc}$$

Where

P_e: is the active power absorbed from the AC system;

P_{eb}: is the active power injected by the inverter to the AC system.

The commands used for the serial inverter are the same for the shunt inverter.

3.3.2. Electricity Grid Modeling

Figure 9 is the model of the electrical network before the disturbance. The alternator is modeled by an ideal generator behind its synchronous reactance, the transformers are modeled as transmission lines whose resistances are negligible, the model of the line did not take into account its resistance and the corona effect and the infinite power network is modeled as a load. Assuming the network is balanced, then the model is single-line. In tables 1 and 2, the data in real and per-uni (pu) sizes are respectively recorded.

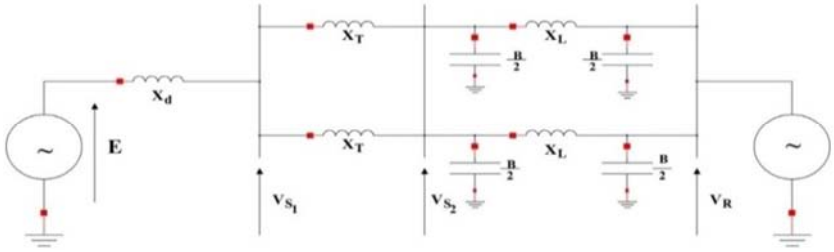

Figure 9. *Model of the electricity network before loss of a term.*

Table 1. *Parameters of network in real values.*

alternator		transformator		Line 220 (kV)		network	
Sn (MVA)	**Un (kV)**	**R (Ω)**	**X (Ω)**	**R (Ω)**	**X (Ω)**	**B (Ω^{-1})**	**Un (kV)**
450	24	0.21	9.4	6	80	$0.6.10^{-3}$	220

Table 2. *Parameters of network in pu.*

alternator		transformator		Line 220 (kV)		network	
Sn (pu)	**Un (pu)**	**R (pu)**	**X (pu)**	**R (pu)**	**X (pu)**	**B (pu)**	**Un (pu)**
4,50	1.05	0.0026	0.1165	0.0484	0.992	0.0744	1.00

Where E is the emf of the alternator;

x_d is the synchronous reactance of the alternator;

Vs1 is the alternator output voltage;

X_T is the reactance of the step-up transformer;

B is the transmittance of the equivalent capacitance formed between conductors and earth;

X_L is the reactance of the line;

R denotes the infinite power network.

The resistances of the alternators, transformers and lines are neglected in front of large values of reactances of this equipment.

The active and reactive power transmissible to the infinite power network are given by the system:

$$\begin{cases} P_{s1r} = \frac{V_{s1}V_r}{X_e} sin\alpha \\ Q_{s1r} = \frac{V_r^2}{X_e} - \frac{V_{s1}V_r}{X_e} cos\alpha \end{cases} \quad (29)$$

3.4. Simulations and Results

3.4.1. Network Simulations Under Normal Operating Conditions and Results

Considering that the network is perfectly compensated to suppose that the voltages at the nodes S and R are respectively 225 and 220 KV, the simulations are made on the basis of the system 26 giving the variations of the active and reactive powers transmissible to the infinite power network in function of α. The results obtained are curves presented in Figures 13 (a) and (b) below.

3.4.2. Post-incident Network Simulations and Results

This time, we still simulate the equations of the system 26 relative network model in Figure 10 below where the line impedance is doubled. The simulations are carried out under the same conditions as above. The results obtained are the curves presented in Figures 12 (a) and (b) below.

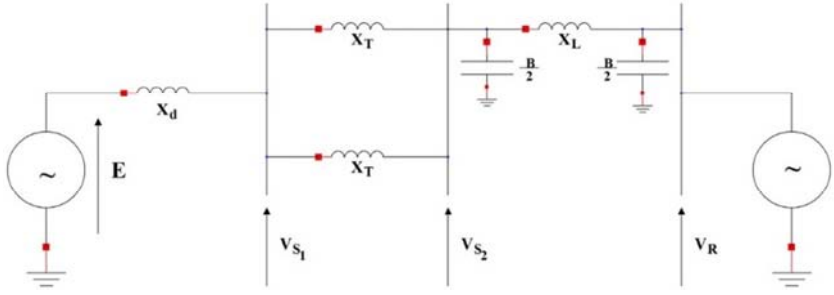

Figure 10. *Model of the electricity network after loss of a term.*

3.4.3. Post-incident Network Simulations Incorporating the UPFC and Results

Here the simulations take into account the incorporation of the UPFC in the absence of existing compensators in order to optimize the transmissible power and regulate the voltage at the interconnection node. The results obtained are curves

presented in Figures 12 (a) and (b) below.

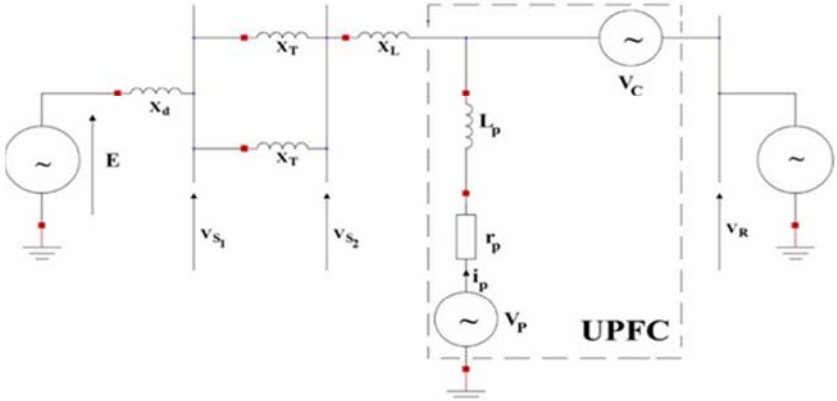

Figure 11. *Model of the electrical network with insertion of the UPFC.*

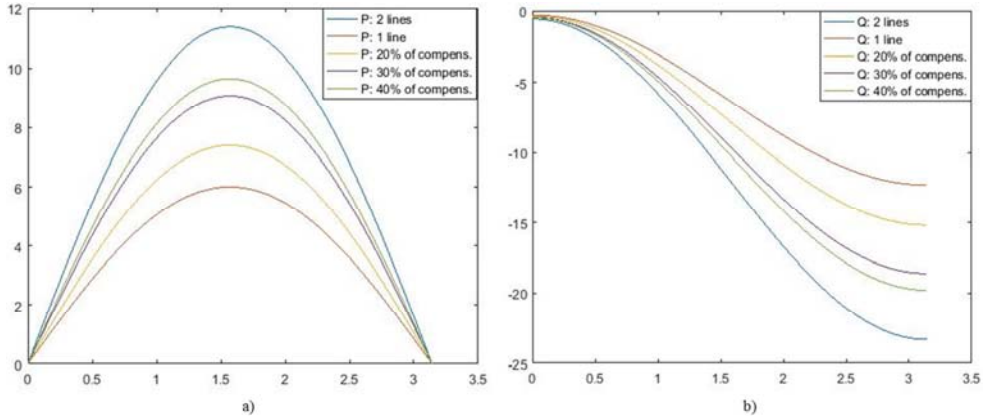

Figure 12. *Variations in active (a) reactive (b) power depending on the angle of transport.*

3.5. Discussion

The curves being obtained; it is necessary to analyze the stability of the network. By applying the criterion of equality of the areas given by the equation 20 and 21 where areaA_1=areaA_2, we note that we are led to solve an equation of the form $acos\delta + b\delta - c = 0$, generally very complex and whose resolution requires numerical methods. However check from the inequality 22 that areaA_1 < areaA_2, to confirm that the system is stable or unstable after this degree of compensation figure 13. Thus we determine areaA_1=67.984 106 w rd and areaA_2=165.31 106 w rd, and therefore the system is stable, because areaA_1 < areaA_2 that is to say 67.984 106 w rd <165.31 106 w rd.

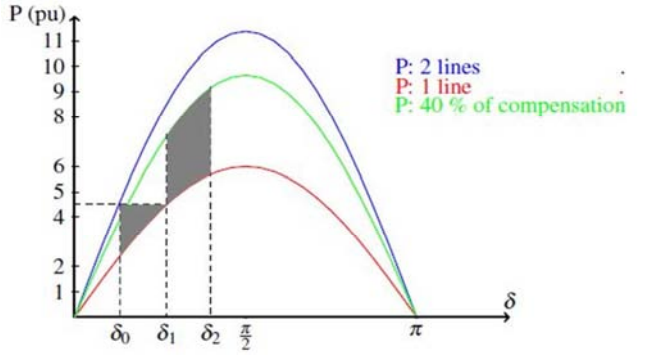

Figure 13. *Criterion of equality of areas justifying the stability of the system.*

4. Conclusion

The study carried out aimed at optimizing the power transit of a line having lost one of these two terms and regulating the voltage at the interconnection node. To do this, we simulated the network before, during and after loss of a term. The simulation after loss of one term saw the insertion of the UPFC which brought a significant improvement in the power flow. The results obtained are interesting, because with a term we obtained the transit of 95% of the initial power by modifying the reactance of the line. Then, we checked that the system is stable after a 45% degree of compensation.

References

[1] Bruno M, Michel. J, Marcs, Outils De Simulation Dynamique Des Réseau Electriques, Technique de l'ingénieur, D 4120-1-22.

[2] Pavella M., Murthy P. G., Transient Stability of Power Systems: theory and practice, Library of Congress Cataloguing in publication, 1994.

[3] Abur A., Exposito A., Power System State Estimation: Theory and Implementation, Marcel-Dekker Inc, 2004.

[4] Arrilaga J., Arnold C. P., Harber B. J., Computer Modeling of Electrical Power System, John Wiley & Sons, 1983, ISBN 0 471 10406 X.

[5] Pai M. A., Energy Function Analysis for Power System Stability, Kluwer Academic Publisher, Boston 1989. ISBN: 0-7923-9035-0.

[6] Xiong K, «Transient Stability of Multimachine Power System with Transfer Conductances», Proceedings of IEEE Intern. Conf. on Cont. Appl., Hartford CT, October 5-7, 1997.

[7] Xue Y., «Fast Analysis of Stability Using EEAC And Simulation Technologies», IEEE Transactions on Power Systems, 1998, p. 12-16.

[8] Wehenkel L., Lebrevelec C., Trotignon M., Batut J. «Probabilistic Design of Power-System Special Stability Controls», Control Engineering Practice, Vol. 7, No. 2, pp. 183-194, 1999.

[9] Matsubara T., Nakamura K., Fujita H., Son M., "Transient Stability Criterion Using Artificial Neural Network", Int. Conf. on Signals Proces. Applic. & Technologies, ICSPAT, Vol. 2, pp. 1204-1208, 1996.

[10] Jean-Claude Sabonnadière et Nouredine Hadjsaïd. Méthodes d'analyse de réseaux électriques. ISBN du volume 2: 978-7462-1642-6 Lavoisier.

[11] Kundur P., Power System Stability and Control, McGraw Hill Inc., 1994, ISBN 0-07-035958-X.

[12] Stephane Gerbex «Metaheuristiques Appliquees Au Placement Optimal De Dispositifs Facts Dans. Un Reseau Electrique»these de doctorat N° 2742 (2003) EPFL.

[13] Zhang P., Coonick A. H., "Coordinated Synthesis of PSS Parameters in multi-machine Power SystemsUsing the method of inequalities Applied to Genetic Algorithms," IEEE Transactions on Power Systems, Vol. 15, No. 2, May 2000, pp. 811-816.

[14] Mathurin GOGOM, Mavie MIMIESSE, Germain NGUIMBI, Désiré LILONGA-BOYENGA. Improving Availability of Transit Capacity by the Hybrid Optimization Method. Journal of Scientific and Engineering Research, 2018, 5 (9): 1-13.

[15] B. LAROUCI, L. BENASLA, A. TAHRI and M. RAHLI. Amélioration de l'influence des variations paramétriques sur les performances de l'UPFC. Volume 53, Number 3, 2012.

[16] Nesmat ABU-TABAK. Stabilité dynamique des systèmes électriques multimachines: modélisation, commande, observation et simulation. Thèse de doctorat soutenue le 19 Novembre 2008.

[17] DJILANI KOBIBI Youcef Islam. Incorporation de l'UPFC dans le calcul de la répartition des puissances dans un réseau électrique. Thèse de doctorat 2016 de l'UNIVERSITE DJILLALI LIABES DE SIDI-BEL-ABBES.

[18] Juan José PASCUAL CAMACHO. Contribution à la modélisation et à la commande d'un UPFC dans le cadre du développement des réseaux intelligents (SmartGrids). Diplôme d'Ingénieur CNAM 2010, CONSERVATOIRE NATIONAL DES ARTS ET METIERS PARIS 2014.